Inelastic Creep-Fatigue Life Evaluation of a Plate-Shell Junction Mock-up

C. Poette

C.E.A., CEN Cadarache, DRNR/STRA, B.P. No. 1, F-13115 St. Paul-lez-Durance, France

G. Cordier

Electricité de France, SEPTEN, 12-14 av. Dutrievoz, F-69628 Villeurbanne Cedex, France

Abstract

A plate-to-shell junction is analyzed as subjected to thermal shocks in sodium without primary loading. The structure is also submitted to 6-hour holding periods at 600°C, and thus sustains creep-fatigue stresses.

After a brief review of the thermal loading conditions of the structure in question, results are presented for various calculations using a bilinear kinematic strain-hardening model. The mean monotonic tensile curve and the cyclic strain hardening curve for the material are used. Other calculations are then presented based on a nonlinear kinematic strain hardening model for which the parameters were identified on stabilized experimental cycles. It is shown that the use of such a model is better suited to the particular structure studied.

Another calculation was also performed involving creep deformation. The resulting stress-versus-time curve is different from the curve obtained under pure relaxation conditions.

1 Introduction and Test Description

This study is part of a program on design rules for structures subjected to high temperature fatigue stresses. The structure and loading studied here are typical of fast breeder reactors: a plate-to-shell junction subjected to repeated cold shocks. Different elasto-plastic models are used to analyse the behaviour of the structure. The results are presented in terms of the number of cycles allowed.

The structure itself consists of a shell 8 mm thick with an outside diameter of 160 mm, and a 10 mm thick tube support plate perforated to permit sodium flow. The structure is not submitted to any primary stress loading. The principles of the thermal loading are shown in Figure 1.

With the structure initially at 600°C, a thermal shock is produced by allowing cooler (350°C) sodium inside the shell on either side of the plate. The mean temperature of the plate thus cooled on both sides is lower than that of the shell, resulting in substantial bending stresses at the plate-to-shell junction: tensile loads on the inside, compression loads on the outside. The radial temperature gradient in the shell also induces similar stresses.

After the thermal shock, the structure is heated to 600°C again and held for 6 hours. Since the elastic limit of the material is exceeded in the junction zone during the thermal shock, reverse stresses appear during the holding period: compression in the groove-ring and tensile loading on the outer face.

The cyclic strains caused by repeated shocks result in fatigue damage; the residual stresses after the 600°C holding period tend to diminish, resulting in creep damage.

2 Thermal Calculations

Thermal calculations were performed using the DELFINE thermal code from the CEA's CASTEM code system. Temperature recordings from the thermal stock experiments on structure mock-ups were available to adjust the limit conditions. For the entire calculation (thermal shock and subsequent reheating) the heat exchange coefficient on the outer surface of the shell was assumed to be 10^3 $W.m^{-2}.°C^{-1}$. For the thermal shock itself, the heat exchange coefficients used were 5000 $W.m^{-2}.°C^{-1}$ for the shell inner wall, and 10^4 $W.m^{-2}.°C^{-1}$ for the plate, while a coefficient of 10^3 $W.m^{-2}.°C^{-1}$ was used throughout for the reheating phase.

Figure 2 compares the experimental and calculated temperature versus time curves during the thermal shock at the points corresponding to thermocouples 3 and 5, representing the shell and the plate, respectively. The computed results are in good agreement with the measured values, and the mechanical calculations can be performed on the basis of the thermal loading determined in this way. Figure 3 shows the computed isothermal lines at the instant of the highest thermal loading, i.e. 5 seconds after the beginning of the thermal shock.

3 Mechanical Calaculations

Mechanical analysis of the test structure was performed using the INCA code from the CASTEM system. Four calculations will be discussed here: three elasto-plastic calculations and one complete inelastic calculation (with allowance for creep deformation).

Figure 4 shows the mesh used for the mechanical calculations. It includes 191 elements (125 eight-node quadrilaterals and 66 six-node triangles) with a total of 606 nodes. Figure 4 indicates two points on the structure designated "groove ring" and "smooth part",which are the most heavily loaded points.

For modeling the material properties, the first two calculations use the linear kinematic strain hardening model; the third uses a Chaboche type nonlinear kinematic strain hardening model; the fourth uses a combined kinematic model for plasticity and a strain hardening creep law.

3.1 First Calculation

This analysis is based on a linear kinematic model derived from a mean monotonic curve at 600°C. The elastic limit and the strain hardening slope were determined from the mean monotonic tensile curve at 600°C modeled by two straight lines. The segment corresponding to the plastic portion passes through the two points on the monotonic curve at abscissa 0.5 and 0.25%. The yield strength is found to be: Sy = 125 MPa.

The calculation was run for two cycles, which is sufficient to ensure good stress and strain stabilization. The following stress values were obtained for the beginning of the high-temperature holding time:

	σ_r (MPa)	σ_z (MPa)	σ_t (MPa)	σ_{rz} (MPa)	$\sigma_{von\ Mises}$ (MPa)	$\Delta\varepsilon$* (%)
Groove ring	-38	-97	-54	+54	107	0.68
Smooth part	2	116	114	0	113	0.22

*$\Delta\varepsilon$ is the quantity equivalent to the total maximum strain sustained during the cycle.

3.2 Second Calculation

The second calculation uses a linear kinematic strain hardening model based on the cyclic curve for the material.The parameters are identified on the consolidated material curve at 600°C,reduced to $\Delta\sigma/2,\Delta\varepsilon/2$. The segment corresponding to the plastic portion passes through the points with abscissa values of $\Delta\varepsilon/2$ = 0.25% and $\Delta\varepsilon/2$ = 0.125%. The yield strength is 128 MPa. The following stresses were obtained:

	σ_r (MPa)	σ_z (MPa)	σ_t (MPa)	σ_{rz} (MPa)	σ von Mises (MPa)	$\Delta\varepsilon$ (%)
Groove ring	-19	-49	-13	26	55	0.48
Smooth part	- 0.9	51	64	- 0.3	58	0.20

3.3 Third Calculation

This calculation uses a Chaboche type nonlinear kinematic strain hardening model with five temperature-dependent variables (R, a_1, c_1, a_2, c_2) and with only kinematic effect. The plasticity surface equation is :

$$R = f(\sigma_{ij}-X_{ij}) = \frac{3}{2} (s_{ij}-X_{ij}) (s_{ij}-X_{ij})^{1/2}$$

where σ_{ij} : stress tensor component

s_{ij} : stress deviator tensor component

X_{ij} : plasticity sphere center tensor component in stress deviator space (i.e. a deviator)

$$X_{ij} = \sum_{l=1,2} X^{l}_{ij}$$

and $dX^{l}_{ij} = c\ (\frac{2}{3}a_l\ d\varepsilon^{p}_{ij} - X^{l}_{ij}\ \ dp)$

where $d\varepsilon^{p}_{ij}$: plastic strain variation tensor component

and $dp = \frac{2}{3}\, d\varepsilon^{p}_{ij}\ .\ d\varepsilon^{p}_{ij}$

R, a_1, c_1, a_2, and c_2 were identified over three stabilized experimental cycles at 600°C, 500°C and 350°C (cycles at $\Delta\varepsilon_T = 0.5\%$). In the calculation, the code values are obtained by linear interpolation between the three temperatures. The following stress values were obtained after three calculations :

	σ_R (MPa)	σ_z (MPa)	σ_T (MPa)	σ_{rz} (MPa)	σ von Mises (MPa)	$\Delta\varepsilon$ (%)
Groove ring	-80	-190	-99	98	198	0.51
Smooth part	0.3	103	130	-0.6	119	0.36

3.4 Fourth calculation

The fourth calculation used a combined kinematic strain hardening model with allowance for creep between cycles. In this model :

$$R = f\ (\sigma_{ij} - \alpha_{ij}) = \frac{3}{2}\ (s_{ij} - \alpha_{ij})(s_{ij} - \alpha_{ij})^{\frac{1}{2}}$$

where α_{ij} : center tensor

$d\alpha_{ij} = \frac{2}{3}c\ d\varepsilon^{p}_{ij}$ where c is determined by the tangent to the material behaviour curve, at its end

$R(\varepsilon p) = \sigma - c\varepsilon p$ where σ : current point on the behaviour curve

εp : cumulative plastic strain

The behaviour curve used is the cyclic curve for the material.
For cyclic loading, the radius R is constant after the first load removal.

The creep law used was identified on the material at 600°C before cycling. Strain hardening is assumed for calculation purposes. No allowance is made for coupling between plasticity and creep. The following values were obtained after three calculation cycles.

	$\sigma_{von\ Mises(1)}$ (MPa)	$\sigma_{von\ Mises(2)}$ (MPa)	$\Delta\varepsilon$ (%)
Groove ring	170*	158*	0.41
Smooth part	107	105	0.19

* Compression stress

(1) Beginning of the third 600°C holding period
(2) End of the third 600°C holding period.

4 Interpretation of Results

The results obtained are illustrated by Figure 5, which shows the limits of the plastic zone from the first calculation, and Figure 6, which shows the von Mises iso-stress map obtained at the end of the third calculation. These are close-up views of the plate-to-sheet junction zone.

The following table summarizes the results obtained, together with service life estimates based on the French RCC-MR code. The following notations are used: N_R = allowable number of cycles; D_f = fatigue damage; D_c = creep damage.

The creep damage estimate for the smooth part is based on the highest principal tensile stress rather than on the conventional von Mises stress. Moreover, for the fourth calculation the estimated service life is specified with and without allowance for stress relaxation during the holding period.

Model	Groove Ring	Smooth Part
1. Linear Kinematics, monotonic curve	$\Delta\varepsilon_T$=0.68% σ_{vM}=107 MPa* N_R=217 D_f=0.87 D_c=0.06	$\Delta\varepsilon_T$=0.22% σ_{Pmax}=116 MPa N_R=1510 D_f=0.15 D_c=0.69
2. Linear Kinematics, cyclic curve	$\Delta\varepsilon_T$=0.51% σ_{vM}=55 MPa* N_R=600 D_f=1 D_c=0	$\Delta\varepsilon_T$=0.13% σ_{Pmax}=105 MPa N_R=2850 D_f=0.16 D_c=0.68
3. Nonlinear Kinematics	$\Delta\varepsilon_T$=0.41% σ_{vM}=198 MPa* N_R=36 D_f=0.07 D_c=0.86	$\Delta\varepsilon_T$=0.2% σ_{Pmax}= 130 MPa N_R=880 D_f=0.06 D_c=0.18
4. Combined Kinematics + creep	$\Delta\varepsilon_T$=0.41% σ_{vM}=170 MPa*§ (3rd cycle) σ_{vM}=158 MPa*§§	$\Delta\varepsilon_T$=0.19% σ_{Pmax}=107 MPa § σ_{Pmax}=105 MPa §§
	N_R D_f D_c	N_R D_f D_c
With creep allowance	134 0.13 0.7	1366 0.07 0.84
w/o stress relaxation	52 0.05 0.89	

* Compression stress - § Beginning of holding period - §§ End of holding period

The results are thus relatively scattered depending on the plasticity models and material characterization curves used. This dispersion can be attributed to different stress estimates for the holding time, directly affecting the creep damage level.

Figure 7 qualitatively accounts for the differences obtained with the first three calculation methods based on uniaxial reasoning. $0-\varepsilon_{max}$ deformation cycles are performed with holding times near $\varepsilon = 0$ (isothermal holding period at 600°C). Under these conditions, the stress level obtained for the holding time with the linear kinematics model depends directly on the strain hardening slope, all other parameters being the same: the higher the slope, the lower the stress level. This explains the otherwise surprising fact that the results obtained using the cyclic curve are less conservative than those obtained with the monotonic curve. The very high stress level obtained using the Chaboche type nonlinear kinematic strain hardening model is attributable to the fact that even with off-center cycles such as $0-\varepsilon_{max}$ the stress loading is relatively symmetrical ($\sigma_{min} \sim -\sigma_{max}$);moreover, this corresponds to actual experimental findings for the high strain levels found in the groove ring ($\Delta\varepsilon_T \sim 0.5\%$). This plasticity model appears better suited for the loading conditions studied here.

No allowance was made in the creep damage estimate with the first three calculation methods for possible stress relaxation between cycles.

The results obtained for the fourth calculation method show the interest of creep calculations for the service life estimate: the permissible number of cycles increases from 52, with no allowance for stress relaxation, to 134 when this is taken into account. Moreover, this estimate is more conservative than if the creep damage were estimated only from the initial stress on the assumption of pure relaxation at each point on the structure. Indeed, this approach would increase the calculated stress relaxation by about 50%. This shows that elastic follow-up is partly involved in the creep phenomenon occurring during the high-temperature holding time.

5 Conclusion

The following conclusions may be drawn from these calculations for the type of structure loading studied :

- A Chaboche type nonlinear kinematic strain hardening model appears to be more suitable for estimating the stress level resulting in creep damage during the holding period.

- Allowance must be made for inter-cycle creep, as it appreciably modifies the service life estimate and cannot be determined by a simple analysis based on a pure relaxation hypothesis. Even in the case of basically secondary loading, when major plastified regions develop they cannot be considered as imposed deformation zones during the creep flow because of certain stress redistribution effects during the high-temperature holding period.

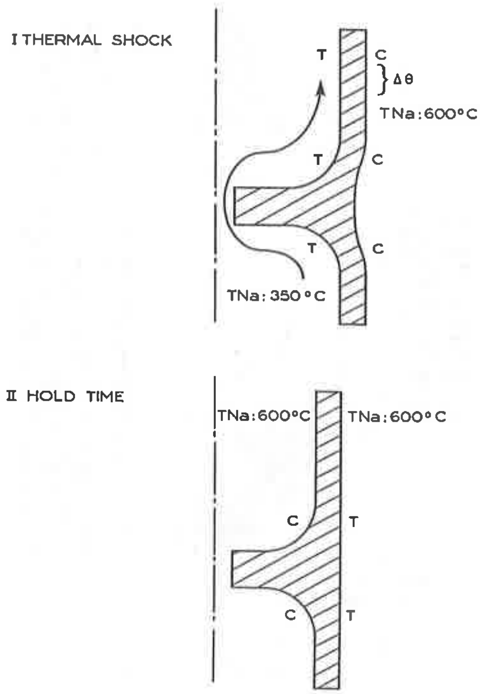

Fig.1: Thermal loading principle

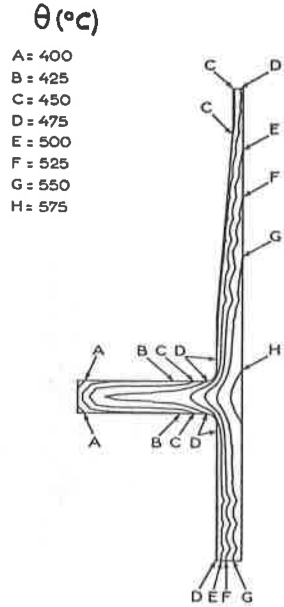

Fig.3: Isothermal lines 5 seconds after the beginning of the thermal shock

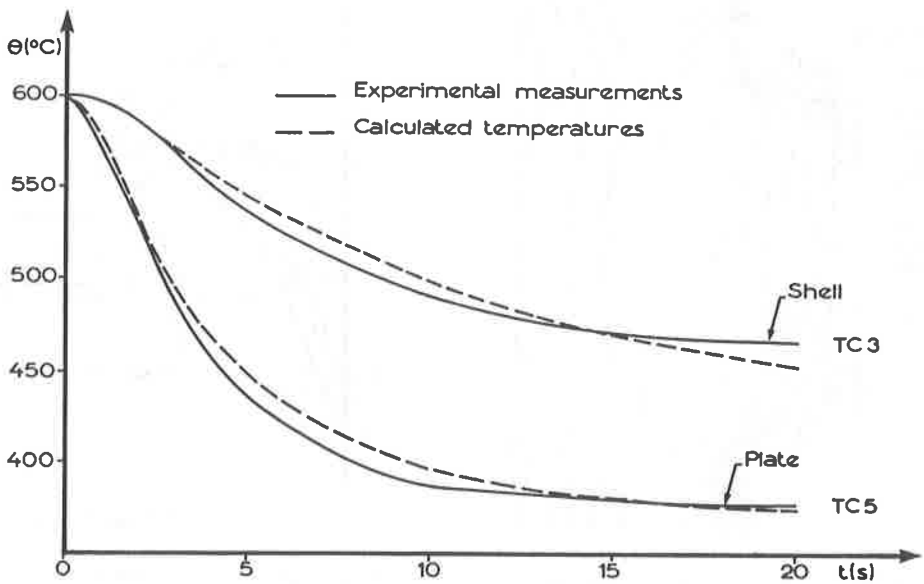

Fig.2: Temperature experimental versus calculated results

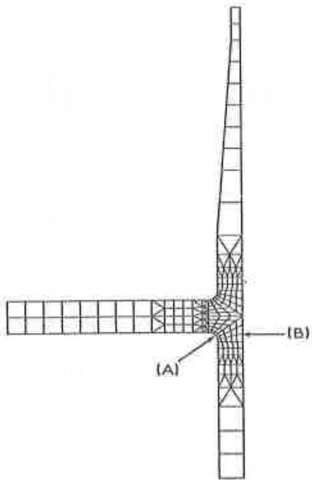

Fig.4: Mechanical calculation mesh

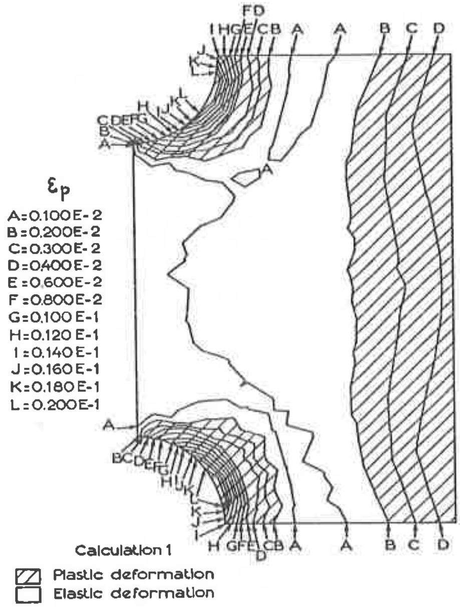

Fig.5: Elastic and plastic zones after the 2nd cycle of the first calculation method

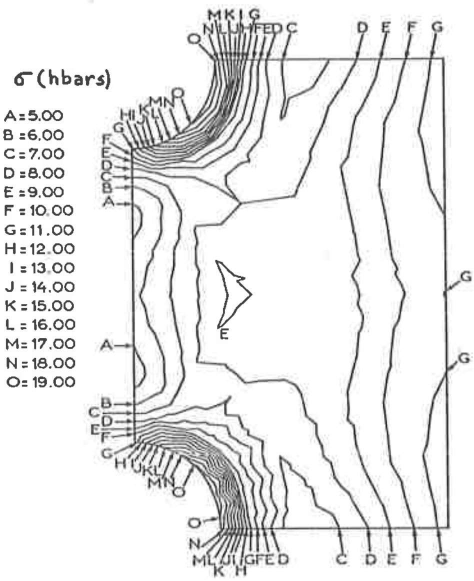

Fig.6: Von Mises iso-stress map for the holding period as computed by the third method

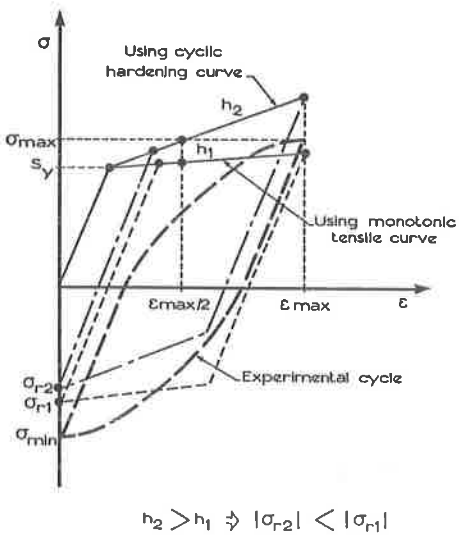

Fig.7: Qualitative interpretation results